Chapter 2
Thermoelectric Properties of Hot-Pressed $K_2Bi_{8-x}Sb_xSe_{13}$ Materials

T. Kyratsi and M. Ioannou

Abstract Alkali bismuth chalcogenides are promising for thermoelectric applications as suggested by previous works. The $K_2Bi_8Se_{13}$ compounds were grown from melt as polycrystalline ingots or from Bridgman technique as highly oriented polycrystalline ingots. In this work, we apply powder techniques as a post-growth process on the $K_2Bi_{8-x}Sb_xSe_{13}$ series and the effect of the sintering process and the Sb concentration on the thermoelectric properties of the series is discussed.

Keywords Sintering • Solid solutions • Structural disorder • Grain boundaries

Introduction

Alkali bismuth chalcogenides attracted considerable attention in the last two decades as candidates for thermoelectrics due to their complex crystal and electronic structure [1]. The properties of $K_2Bi_8Se_{13}$-based compounds were studied in more detail as the most promising. The properties of materials grown from melt as polycrystalline ingots [2, 3] or from Bridgman technique as highly oriented polycrystalline ingots have been reported in several publications [4, 5]. Powder techniques were applied as post-growth methods through pressureless sintering [6, 7] and also, only recently, through hot pressing [8] on $K_2Bi_8Se_{13-x}S_x$ series. The hot-pressed pellets had high density and performed ZT of about 0.5 at 800 K.

In this system, the formation of solid solutions has been extensively studied as a common strategy to minimize the thermal conductivity and there are several reports on substitution at the heavy metal sites, i.e., $K_2Bi_{8-x}Sb_xSe_{13}$ [4, 9], the chalcogenide sites, i.e., $K_2Bi_8Se_{13-x}S_x$ [10]; as well as the alkali metal sites, i.e., $K_{2-x}Rb_xBi_8Se_{13}$ [11].

T. Kyratsi (✉) • M. Ioannou
Department of Mechanical and Manufacturing Engineering, University of Cyprus, 1678 Nicosia, Cyprus

A. Amaldi and F. Tang (eds.), *Proceedings of the 11th European Conference on Thermoelectrics: ECT 2013*, DOI 10.1007/978-3-319-07332-3_2,

Crystallographic studies show that the nonuniform partial substitution of Bi/Sb decreases the lattice thermal conductivity [12] but also significantly affects the electronic properties through changes in structural disorders [5].

In this work, we apply post-growth powder techniques on the Sb series and hot-pressed pellets of $K_2Bi_{8-x}Sb_xSe_{13}$ ($0 \leq x \leq 2.4$) are fabricated. The hot pressing conditions were selected based on the previously applied statistical design of experiments optimization approach [8]. The effect of the sintering process and the Sb concentration on the thermoelectric properties of the series is discussed. A comparison with different types of samples, prepared also by post-growth techniques (i.e., oriented polycrystalline ingots), is also presented.

Experimental Section

Chemicals were used as obtained: potassium metal, rod, 99.5 % purity, Sigma Aldrich, and bismuth, antimony, and selenium metals, 99.999 % purity from Alfa Aesar and all manipulations during synthesis were carried out under a dry argon atmosphere in an MBraun glovebox. The $K_2Bi_{8-x}Sb_xSe_{13}$ series was synthesized in the form of ingot as explained in the following: mixtures of elements were weighted according to the chemical formula of each member and were sealed in silica tube under pressure of $<10^{-5}$ Torr. The mixtures were, then, heated to 850 °C over 12 h and kept there for 1 h, followed by cooling to 50 °C at a rate of −15 °C/h. The ingots were broken in small pieces and ground using a mortar and pestle. Pellets were fabricated using a uniaxial hot-press system (HP20) from Thermal Technologies Inc. The sintering conditions were modified according to each member's melting point as discussed below.

The samples were examined by X-ray powder diffraction to assess phase purity. Powder patterns were obtained using a Rigaku Miniflex powder X-ray diffractometer with Ni-filtered Cu Ka radiation operating at 30 kV and 15 mA. Seebeck coefficient and electrical conductivity measurements were carried out on the hot-pressed pellets simultaneously using a commercial ZEM-3 system from ULVAC-RIKO. A Netzsch LFA-457 system was used to measure thermal diffusivity and heat capacity. The diffusivity (D), density (ρ), and specific heat (C_p) were measured and used to calculate the total thermal conductivity using the formula $\kappa = D \times \rho \times C_p$.

Results and Discussion

Synthesis and Pellet Fabrication

Selected members of $K_2Bi_{8-x}Sb_xSe_{13}$ series were synthesized and hot pressed into pellets. The final products were single $K_2Bi_8Se_{13}$ phase as concluded by powder X-ray diffraction (PXRD). The sintering conditions were selected based on the

Table 2.1 Melting point (T_{MP}) and sintering conditions (hot-pressing temperature (T_{HP}), pressure (P), and time at maximum temperature) of the $K_2Bi_{8-x}Sb_xSe_{13}$ materials

x	T_{MP} (°C)	T_{HP} (°C)	P (MPa)	Time (min)
0.0	700	540	80	90
0.8	687	530	80	90
1.6	675	520	80	90
2.4	654	505	80	90

results of the previously reported optimization process [8]. However, the actual sintering temperatures had to be adjusted due to the different melting points of the Sb members. Table 2.1 shows the sintering conditions and melting points [4] for each stoichiometry. The relative densities of the hot-pressed pellets were between 94 and 98 %.

Electrical Conductivity and Seebeck Coefficient

It is the first time that members of the $K_2Bi_{8-x}Sb_xSe_{13}$ series are processed via powder techniques, i.e., grinding and sintering with hot pressing; therefore a comparison with the highly oriented ingots previously studied is attempted. Figure 2.1a shows that the electrical conductivity values of the members prepared as highly oriented polycrystalline ingots by Bridgman technique [5] are much higher than those reported here. Since the hot-pressed pellets include many grains and the boundaries significantly decrease the mobility of the carriers, such behavior was expected. In addition, the anisotropy of this system is well known and affects the thermoelectric properties along and perpendicular to the needle orientation (crystallographic *b*-axis). The electrical conductivity along the needle direction was found to be five times higher than the perpendicular one [4]. Therefore, the contribution of the different crystallographic directions is also involved here, although this does not seem to be the main mechanism here.

On the other hand, the Seebeck coefficient of the pressed pellets is higher, in absolute values, than the reported values for oriented ingots; see Fig. 2.1b. This suggests lower carrier concentration that could be explained by the fact that the post-growth processes were different; hot pressing is a solid-state process at lower temperatures while the oriented ingots were prepared after melting the materials at higher temperatures. The variation of the Seebeck coefficient due to anisotropy is less important as discussed in ref. [4].

According to previous work on polycrystalline oriented ingots [5], the behavior of the Bi-rich members is that of typical heavily doped semiconductors. For the hot-pressed pellets, this is also the case for the member $x=0$; see Figs. 2.2 and 2.3. When Sb incorporates in the lattice the electron concentration decreases. At the same time, the temperature dependence of the electrical conductivity changes with Sb and this can also be attributed to the lower carrier concentration. The electrical

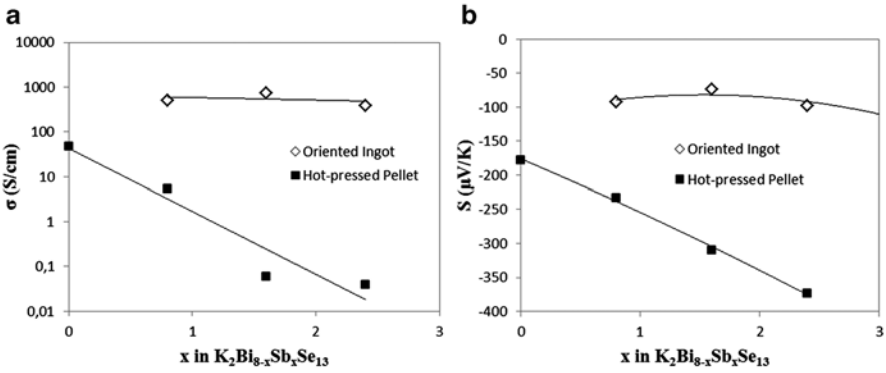

Fig. 2.1 (**a**) Electrical conductivity and (**b**) Seebeck coefficient of $K_2Bi_{8-x}Sb_xSe_{13}$ hot-pressed pellets in comparison to materials prepared as oriented ingots [5]

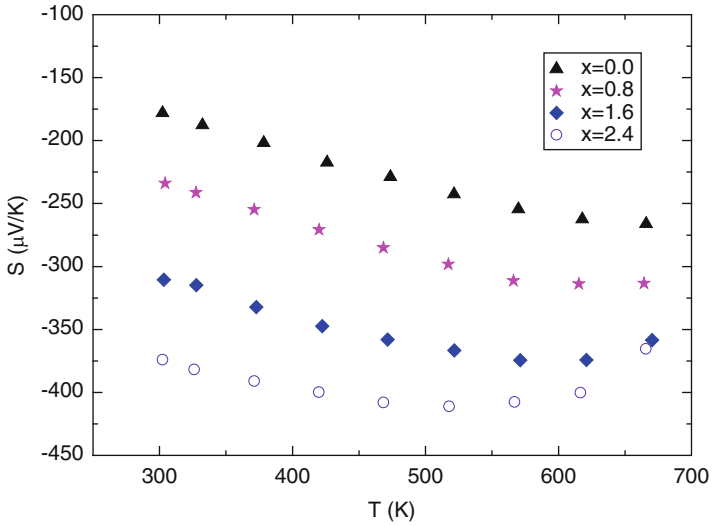

Fig. 2.2 Temperature dependence of Seebeck coefficient of $K_2Bi_{8-x}Sb_xSe_{13}$ hot-pressed pellets

conductivity in this temperature range changes from that of typical heavily doped semiconductors to intrinsic semiconducting region.

In order to better understand the properties, one should have a closer look on the crystal structure. $K_2Bi_8Se_{13}$ material has a complex structure, as shown in Fig. 2.4, that includes two different interconnected types of Bi/Se building blocks and K^+ atoms in tunnels. The two different Bi/Se blocks are connected to each other at special mixed-occupancy K/Bi sites that seem to be crucial in defining the electronic structure near the Fermi level and consequently the electronic properties. This is supported by ab initio density functional band structure calculations on this material [13].

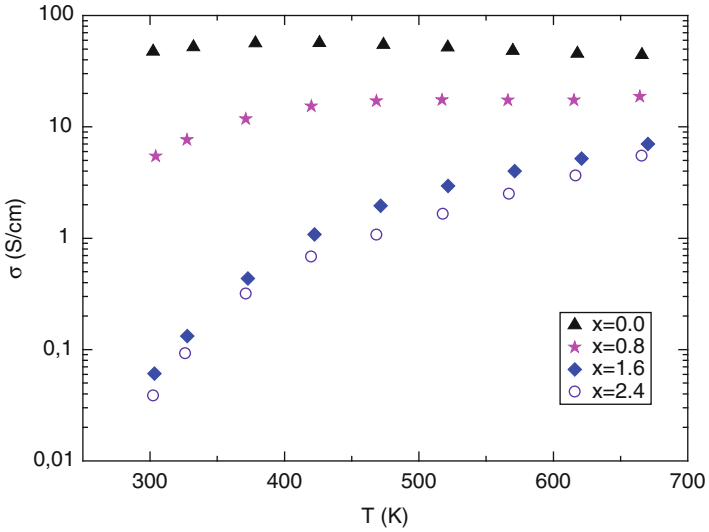

Fig. 2.3 Temperature dependence of Seebeck coefficient of $K_2Bi_{8-x}Sb_xSe_{13}$ hot-pressed pellets

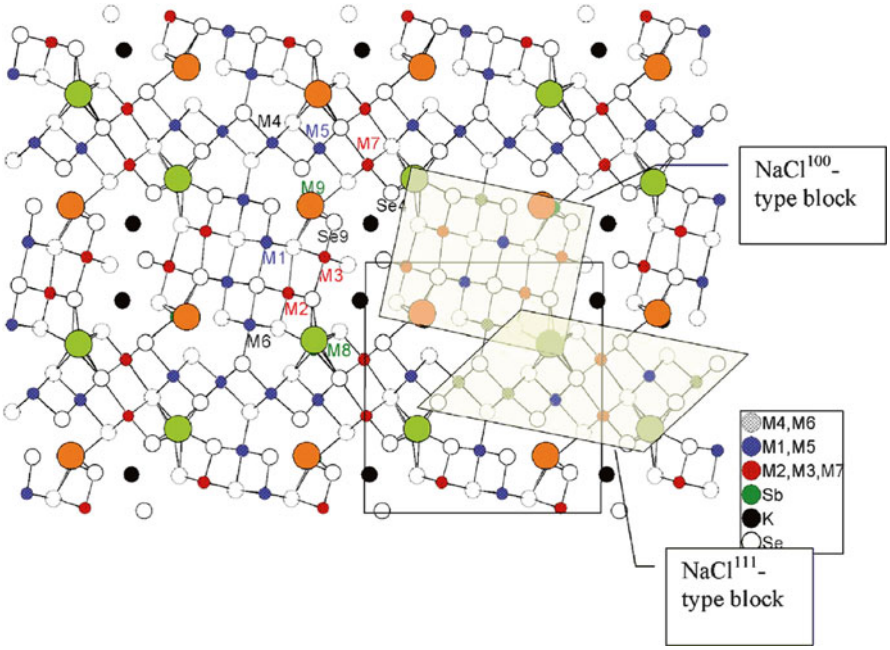

Fig. 2.4 Crystal structure of $K_2Bi_8Se_{13}$ compound (from ref. [5])

As discussed previously regarding the ingots [5], the incorporation of Sb affects the properties in two different ways, one related to these mixed-occupancy sites mentioned above. The band structure calculations on $K_2Bi_8Se_{13}$ dealt with the mixed occupancy of the *M*/K sites *M*(8) and *M*(9) [13]. The occupancy of the *M*(8) and *M*(9) was once considered to exclusively contain either K or Bi atoms and according to band structure calculations this led to semimetallic behavior with $Eg = 0$. In another case, a $1 \times 2 \times 1$ supercell with ordered Bi and K distributions was involved and the band structure calculations showed a semiconductor with $Eg = 0.55$ eV, a value close to the experimental gap of 0.60 eV. When Sb is introduced in the lattice, it preferentially occupies the sites *M*(8) and *M*(9) (Fig. 2.4) until *x* reaches 1.5 or 1.7 [5]. At higher concentration, the additional Sb atoms show again a preferential substitution for the sites with distorted octahedral coordination environment which are proximal to the mixed sites *M*(8) and *M*(9) and these are *M*(2), *M*(3), *M*(7), *M*(1), and *M*(5); see Fig. 2.4 [5]. Since the donors originate from the degree of order/disorder at the mixed-occupancy M/K sites, the gradual elimination of the disorder with the Sb incorporation reveals a more semiconducting character of the $K_2Bi_{8-x}Sb_xSe_{13}$ materials. This is in agreement with our results in oriented ingots [5] as well as the hot-pressed pellets in this work.

On the other hand, there is a variation of the energy band gap of the compounds that affect the properties [4]. The energy gaps of the end members $K_2Bi_8Se_{13}$ and $K_2Sb_8Se_{13}$ are 0.59 eV and 0.78 eV respectively [2]. However, the gaps of the $K_2Bi_{8-x}Sb_xSe_{13}$ series do not increase monotonously, as expected, but small amounts of Sb actually cause the *Eg* to slightly decrease and it actually increases only when Sb atoms replace 30 % of Bi atoms ($x \approx 2.5$) [4].

In the case of the hot-pressed pellets, all the above phenomena are valid and can explain the variation in the properties with Sb concentration. The elimination of the structural disorder as well as the small changes in the energy gap are expected to affect the properties in the hot-pressed pellets in the same way as previously observed in oriented ingots. On the other hand, differences such as the lower doping level, can be understood in terms of the different type of the applied post-growth process (hot press as solid-state process vs. melting).

Thermal Conductivity and Figure of Merit

Thermal conductivity measurements of the members of the $K_2Bi_{8-x}Sb_xSe_{13}$ series are shown in Fig. 2.5. The room-temperature values are between 0.30 and 0.6 W/m K which are very low compare to other thermoelectric materials. For $x = 0$ the thermal conductivity value is lower than that of 1.28 W/m K [2] that corresponds to highly oriented polycrystalline ingot, but it is similar to that of 0.3 W/m K, expected for pressed pellet [14] and these differences can be explained based on the anisotropy of these materials and the porosity as discussed elsewhere [14]. The lattice thermal conductivity seems to be the major contribution to the total thermal conductivity

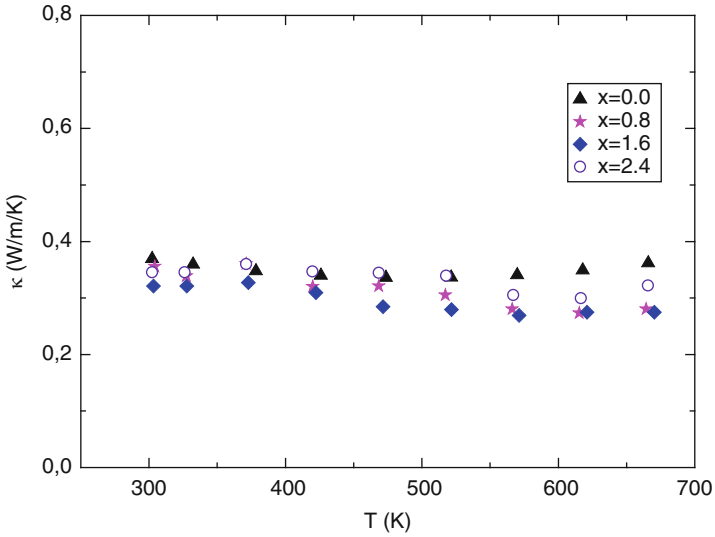

Fig. 2.5 Temperature dependence of thermal conductivity of $K_2Bi_{8-x}Sb_xSe_{13}$ hot-pressed pellets

due to the low electrical conductivity values and correspond to values of 0.32–0.35 W/m K. These values are very similar to those of $K_2Bi_8Se_{13-x}S_x$ pellets [8]. The figure of merit ZT was maximum for the $x=0$ member reaching 0.58 at 673 K. For higher x values the maximum ZT decreased to 0.43, 0.22, and 0.15 for the members $x=0.8$, 1.6, and 2.4, respectively.

Conclusions

In this work, hot-pressed pellets of the $K_2Bi_{8-x}Sb_xSe_{13}$ series were prepared for the first time. The sintering conditions followed previous results based on statistical design of experiments approach and were modified based on the different melting point of the compounds. The pellets prepared by hot pressing presented different properties than those previously reported for oriented polycrystalline ingots and these can be understood based on the different post-growth processes applied in each case (solid-state process vs. melting). The electrical conductivities were significantly lower as expected due to the contribution of the grain boundaries, while the Seebeck coefficient measurements suggested lower doping level in these materials. Regarding the thermal conductivity, all members exhibited very low values due to the combination of the complex crystal structure of the materials and the powder processing. More work is in progress trying to modify the electronic properties as well as keep the benefit of this extremely low thermal conductivity.

Acknowledgments This work was co-funded by the European Regional Development Fund and the Republic of Cyprus through the Research Promotion Foundation (Infrastructure Project ΑΝΑΒΑΘΜΙΣΗ/0308/17).

References

1. Kanatzidis MG (2000) Semiconduct Semimet 69:51
2. Chung D-Y, Choi K-S, Iordanidis L, Schindler JL, Brazis PM, Kannewurf CR, Chen B, Hu S, Uher C, Kanatzidis MG (1997) Chem Mater 9:3060
3. Kyratsi T, Kika E, Hatzikraniotis E, Paraskevopoulos KM, Chrissafis K, Kanatzidis MG (2009) J Alloys Compd 474:351–357
4. Kyratsi T, Dyck JS, Chen W, Chung D-Y, Uher C, Paraskevopoulos KM, Kanatzidis MG (2002) J Appl Phys 92(2):965
5. Kyratsi T, Hatzikraniotis E, Paraskevopoulos KM, Malliakas CD, Dyck JS, Uher C, Kanatzidis MG (2006) J Appl Phys 100:123704
6. Tsiappos A, Kyratsi Th, Kanatzidis MG (2006) Proceedings of 25th international conference on thermoelectrics, IEEE, pp. 516–519
7. Tsiappos A, Kyratsi Th, Hatzikraniotis E, Paraskevopoulos KM, Kanatzidis MG (2007) Proceedings of 5th European Conference on Thermoelectrics, Ukraine
8. Kyratsi T, Ioannou M (2013) J Electron Mater 42:1604
9. Kyratsi T, Chung D-Y, Kanatzidis MG (2002) J Alloy Comp 338:36–42
10. Kyratsi T, Kanatzidis MG, Anorg Z (2003) Allg Chem 629(12):2222–2228
11. Kyratsi T, Chung D-Y, Ireland JR, Kannewurf CR, Kanatzidis MG (2003) Chem Mater 15:3035–3340
12. Kyratsi T, Hatzikraniotis E, Paraskevopoulos KM, Dyck JS, Shin HK, Uher C, Kanatzidis MG (2004) J Appl Phys 95(8):4140
13. Bilc D, Mahanti SD, Kyratsi T, Chung D-Y, Larson P, Kanatzidis MG (2005) Phys Rev B 71(8):085116
14. Kyratsi T, Hatzikraniotis E, Ioannou M, Chung DY, Tsiaoussis I (2011) J Appl Phys 110:033713
15. Chung D-Y, Iordanidis L, Choi K-S, Kanatzidis MG (1998) Bull Kor Chem Soc 19:1281–1293
16. Kanatzidis MG (ed) (2003) New thermoelectric materials workshop chemistry, physics and materials science of thermoelectric materials: beyond bismuth telluride, fundamental materials science series. Kluwer Academic/Plenum, New York

http://www.springer.com/978-3-319-07331-6

Proceedings of the 11th European Conference on Thermoelectrics
ECT 2013
Amaldi, A.; Tang, F. (Eds.)
2014, XVII, 228 p. 130 illus., 99 illus. in color.,
Hardcover
ISBN: 978-3-319-07331-6